

Mapping Magnetisation using a Magnetoencephalography System

Richard Bowtell¹, Mobeen Ali¹, Jason Medica¹, Ingrid Vella¹, and Matthew Brookes¹
¹School of Physics and Astronomy, University of Nottingham, Nottingham, United Kingdom

PURPOSE: There is increasing interest in the development of ultra-low field (ULF) MRI systems that use SQUIDS for detection of the NMR signal¹⁻³. ULF MRI offers a number of benefits, including: low cost, strong contrast because of the increased relative dispersion of T1 relaxation times⁴, and the potential for carrying out magnetoencephalography (MEG) and MRI using the same system^{1,2}. Although significant success has been achieved in implementing MRI at ULF, the use of non-inductive detection schemes in conjunction with the time-varying magnetic fields needed for imaging transverse magnetisation is not straightforward, because of the sensitivity of the detectors to magnetic field changes. After pre-polarisation it might also be possible to detect the decaying, longitudinal, nuclear magnetization using SQUID magnetometers. An image of the magnetization distribution could then be formed by solving the inverse problem relating the magnetization distribution to the magnetic fields produced at an array of sensors. With this approach, the pre-polarisation needed to enhance the magnetization relative to the thermal polarization available at ULF, can be carried out at a distance from the MEG scanner and no field gradients need be applied. The detector array consequently does not have to be exposed to any time-varying fields. This approach can be implemented on an unmodified MEG system using a simple, permanent magnet arrangement to provide the ULF needed for detection. Here, we describe initial experiments demonstrating the feasibility of using an MEG system to detect and image decaying longitudinal nuclear magnetization from pre-polarised aqueous samples. We also show that an MEG system can be used to map susceptibility-related magnetization induced in samples exposed to ULF.

METHODS: Experiments were carried out using a 275-channel MEG system (MISL, BC, Canada) which uses axial gradiometers with 5 cm baseline, as well as higher order synthesised gradients for interference rejection. A sample holder with 5 slots that could each accommodate a plastic bottle (6 cm length, 4 cm diameter) was fixed inside the MEG helmet. Fiducial coils were affixed to the sample holder to allow its position to be measured relative to the detector array, for subsequent co-registration of magnetization images with MRI data characterising the sample holder geometry. The ULF for imaging was generated by a cylindrical permanent magnet (6.5 cm dia.; 7 cm length) positioned at a distance of 2 m axially from the sample holder. This magnet, which had a dipole moment of 215 Am², could be freely rotated in a horizontal plane so as to vary the magnitude and direction of the imaging field. With the magnet oriented parallel (0° or 180°) or perpendicular (90° or 270°) to the axis, the field was correspondingly directed with a strength of 5.5/2.75 μ T (varying by less than 4% in magnitude and 5° in orientation over the samples). In initial experiments, we measured the magnetic fields produced when a sample of 9.67 g of powdered manganese sulphate monohydrate (MnSO₄·H₂O) was inserted into one of the five slots in the sample holder. Subsequently, bottles containing 78 ml of water doped with varying amounts (0 – 20 μ M) of Gadoteridol were polarised for 180 s, using one or more 0.2 T permanent magnets (4 cm gap and 4.8-cm-diameter pole pieces), sited just outside the magnetically shielded room housing the MEG system. Magnetic field recordings of 60s duration were made with samples transferred manually from the polarising magnet into the sample holder at t ~ 20 s. The transfer process took around 3-4 s. Three-dimensional maps of the magnetization distribution (8 mm isotropic voxels) were calculated from the magnetic fields measured at the sensors using an adapted version of the dynamic Statistical Parametric Mapping (dSPM)⁵ approach that is commonly used in MEG. This is a least squares approach which minimises the error between the measured and modelled fields, and the norm of the magnetization distribution. The weighting parameters are also normalised to produce a uniform spatial distribution of noise in the solution. The lead fields were generated using standard expressions for the magnetic field produced by a unit dipole and the output is a pseudo-Z score reflecting the magnetization distribution. *A priori* knowledge of the direction of the imaging field meant that it was possible to constrain the dSPM solution, by pre-defining the orientation of nuclear magnetization. Weighted fits of the exponential decay of the magnetization and associated magnetic fields were used to find the T₁ of the samples.

RESULTS: Figure 1 shows maps of the magnetic fields generated with MnSO₄ located in three different slots of the sample holder with the imaging field at 180°. These fields, which have peak values of -15 pT show the expected dipolar signature and track the sample location. Corresponding dSPM volumetric images thresholded at 90% of their maximum values, are also shown overlaid on MRI data. Figure 2 shows a map of the magnetic field produced immediately after a pre-polarised water sample was placed in the leftmost slot of the sample holder, with the imaging field at 0°. The insets show the temporal variation of the measured field at two MEG sensors. A peak field of around 4 pT is generated, with a pattern consistent with a dipole oriented in the z-direction. Fitting the decay of the magnetization across sensors yielded a T₁ value of 2.4 s. Figure 3 shows one coronal slice of a magnetisation map obtained when fields from two, pre-polarised samples of distilled water (one doped with 5 μ M Gadoteridol) were simultaneously measured. Reduced magnetization resulting from the faster decay in the doped sample, whose T₁ was measured to be 1.3 s, is evident.

DISCUSSION The net magnetic moment of the 9.7g of MnSO₄ ($\chi_m = 0.178 \text{ mole}^{-1}[\text{SI}]$) is 56 nAm² in a magnetic field of 5.5 μ T, yielding a peak radial field change on a 5 cm baseline of 17 pT at an 8 cm distance – consistent with the maximum measured field of ~15 pT (Fig.1), while 78 ml of water polarised at 0.2 T at 300 K has a magnetic moment of 50 nAm², which would reduce to around 14 nAm² after 3 s of relaxation with T₁ = 2.4 s consistent with the ~4-fold smaller field measured from the pre-polarised distilled water compared to the MnSO₄ (Figs. 1 and 2). We have shown that applying the dSPM approach to field measurements recorded from a 275-channel MEG scanner yields reasonable quality images of a three-dimensional distribution of magnetisation with around 0.1 nAm² per voxel and that that these images are consistent with the geometry of the sample holder identified from MRI. Further work is needed to optimise solutions of the inverse problem for dipolar lead fields and to establish the best achievable resolution. Imaging nuclear magnetization in biological systems using this approach will require speed up of the transfer from the pre-polarisation magnet into the MEG scanner, because of the short relaxation times of such systems at low field. It has been proposed that BOLD effects⁶ could be measured in human subjects in ULF by using SQUID magnetometers to monitor susceptibility changes. Our measurements on MnSO₄ samples show that the dSPM method may be usefully applied in this context.

REFERENCES: (1) Zotev et al., JMR 2008. **194** :115 (2) Vesanen et al., MRM, 2013. **69**: 1795 (3) Inglis et al., PNAS, 2013. **110**: 19194. (4) Michalak et al., MRM 2011 **66** 605. (5) Dale et al., *Neuron*, 2000. **26**: 55. (6) Burke and Diamond, *Physiol. Meas.*, 2012. **33** 2079.

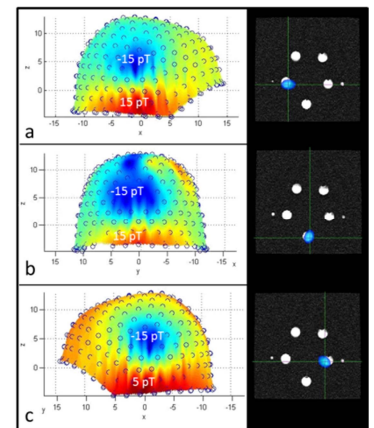


Figure 1: (Left) Maps of magnetic field due to MnSO₄ sample in 3 different slots (a-c) of sample folder. (Right) Corresponding thresholded magnetization maps in one axial slice.

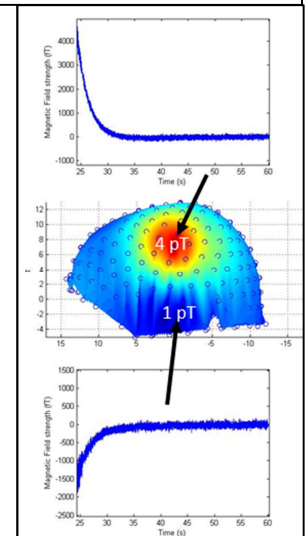


Figure 2: Map of magnetic field due to pre-polarized water; temporal variation of field at 2 sensors.

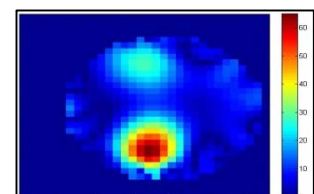


Figure 3: Magnetization map from two pre-polarized aqueous samples (top- doped; bottom - undoped)